Experimental Techniques (2018) 42:631–644
https://doi.org/10.1007/s40799-018-0286-6

Experimental Investigations and Parametric Optimization of Process Parameters on Shrinkage Characteristics of Selective Inhibition Sintered High Density Polyethylene Parts

D. Rajamani [1] · E. Balasubramanian [1] · P. Arunkumar [1] · M. Silambarasan [1] · G. Bhuvaneshwaran [1]

Received: 19 May 2018 / Accepted: 30 August 2018 / Published online: 7 September 2018

Abstract
Fabrication of functional prototypes from computer-aided design data through joining polymer powders particles is accomplished using selective inhibition sintering (SIS) process. The dimensional accuracy of sintered specimens in SIS process is significantly affected for the materials such as polymer and inhibitor, complex geometry and process parameters. Increasing dimensional accuracy in SIS process improves the quality and functional ability of end-use components. The present work investigates the shrinkage characteristics of SIS parts with reference to various process parameters such as thickness of layer, heater energy and its feedrate, and inhibitor nozzle feedrate. The test specimens are fabricated using the developed SIS system. Experimental study and mathematical modelling is accomplished based on statistical box-behnken response surface methodology. The result of analysis of variance (ANOVA) revealed that the layer thickness followed by printer feedrate and heater feedrate are the dominating variables on shrinkage. The optimal operating conditions of selected process variables to reduce shrinkage is presumed using desirability approach. The results revealed that the settings of low layer thickness and high heater energy with medium heater feedrate and medium printer feedrate is beneficial for improving dimensional stability of sintered specimen. Furthermore, the effect of these parameters on shrinkage are evaluated by conducting sensitivity analysis.

Keywords Additive manufacturing · Selective inhibition sintering · High density polyethylene · Shrinkage · Desirability · Sensitivity

Introduction

Rapid Prototyping (RP) is a disruptive technology to realise computer aided design (CAD) parts in short span of time. The traditional subtractive manufacturing processes may increase the cost burden and huge human effort is required to manufacture the part [1]. However, the RP processes have the capability to generate intricate 3D parts without usage of tooling and lead time of the product can be reduced up to 50% [2, 3]. Owing to the peculiar characteristics of RP processes such as cost-effective, time efficient, and can handle diversity of materials such as metals, ceramics and thermoplastics [4], they have gained an extensive attention in the fields of automotive, aeronautical, medical and custom consumer products [5]. In the past decades, several RP processes such as stereolithography (SL), fused deposition modelling (FDM), direct metal deposition (DMD), selective laser sintering (SLS) and three-dimensional printing (3DP) have been developed. Each RP process is varied with reference to layer deposition, principle of operation, and usage of materials [6]. However, they have few common processing steps including building of CAD models, slicing, machine tool-path generation, and post-processing.

Out of available rapid prototyping processes, Selective Inhibition Sintering (SIS) [7] is considered to be an innovative and economical RP technique that fabricates parts on a layer-upon-layer basis. In this process, polymer powder particles are sintered with desired part profiles which are defined through precise delivery of inhibitors. Adaptability to various materials such as polymers, ceramics and metals is one of the key advantages of SIS process. It can also utilize indigenous polymers and metal powders that makes the system cost effective [8]. The step-by-step procedure to fabricate the parts are:

✉ D. Rajamani
rajamanitamil1991@gmail.com

[1] Centre for Autonomous System Research, Department of Mechanical Engineering, Vel Tech Rangarajan Dr. Sagunthala R&D Institute of Science and Technology, Chennai 600062, India

1. First layer is formed through spreading the powder on the build platform with an aid of rollers
2. Delivery of inhibitor at the part boundaries using a nozzle which moves along the formed layer. The numerical control (NC) tool path is generated from the software based upon the solid model.
3. Sintering of powder layer is achieved using a low cost heater.
4. The above three steps are reiterated until the final part is made. The prototyped part is removed from the build chamber and surplus powder is deposited into the recycle tank.

The commercialization of SIS system is still cumbersome due to compatibility issues with reference to NC tool path generation, powder compaction, reducing powder wastage and optimization of SIS process variables. Hence, it is vital to realize the inadequacies of a process to meet the demands of numerous applications. It has been suggested that enrichment of dimensional accuracy, specimen strength, surface quality and built time are the crucial disputes to be addressed for effective implementation of rapid prototyping technology [9].

Several studies have been made to enhance the quality and performance characteristics of RP parts through appropriate selection of process variables. Mahapatra et al. [10] have identified that raster width followed by thickness of each layer and part orientation are the most influencing variables on surface quality of FDM parts. Sachdeva et al. [11] explored the consequence of process variables on surface quality of SLS parts utilizing response surface methodology (RSM). They have found that input energy for laser and scan spacing are critical variables in affecting the surface finish. Sood et al. [12] have considered FDM part to investigate the compressive strength using particle swarm optimization and artificial neural network approach. They found that the compressive strength of fabricated parts are abridged due to anisotropy properties of polymers and weak interlayer bonding due to the formation of pores. Rayegani et al. [13] have performed experiments on improving the tensile strength of FDM parts. They proposed a differential evolutionary approach to examine the tensile strength which is significantly influenced by combination of negative air gap, smaller raster width, and increased raster angle. Rajamani et al. [14] fabricated high density polyethylene parts using SIS system and evaluated mechanical strength of sintered parts using response surface approach. Their results revealed that, mechanical strength of specimens is improved through increasing heater energy and reducing thickness of powder layer. Balasubramanian et al. [15] evaluated wear properties of high density polyethylene parts produced using SIS process and investigation on the influences of SIS variable is performed.

One of the major challenges in parts produced by RP process is to achieve the dimensional accuracy as it is a function of many factors such as process parameters, powder properties, tessellation from the computer aided 3D model, slicing algorithm, part geometry and shrinkage [16]. Several researchers have attempted to enhance the dimensional precision of RP parts by adjusting the consequence of shrinkage. Singh et al. [17] proposed RSM based central composite design to optimize the process parameters on selective laser sintering process. They have reported that the scan spacing and the laser power are the most influencing parameters which affected the shrinkage of SLS parts. Further, increase in scan spacing has reduced the shrinkage, whereas increase in laser power escalate the shrinkage comparatively. Sood et al. [18] utilized a hybrid grey-taguchi technique to investigate the shrinkage of FDM parts. They have proposed that the thickness of FDM parts increased due to the growth of predominant shrinkage in length and width. Negi et al. [19] used artificial neural network (ANN) and RSM on accounting shrinkage behaviour of PA 3200GF specimens. They found that ANN technique predicts better optimum solution in comparison to RSM and great influence on shrinkage is observed through varying scan speed, scan spacing and part bed temperature. Senthilkumaran et al. [20] stated that directional impact due to specimen orientation and scan length has more influence on shrinkage of SLS parts. Also, shrinkage is less and highly non-uniform in the direction of scanning in comparison to its orthogonal scanning direction. Wang et al. [21] used neural network to examine the influence of SLS variables on shrinkage characteristics of sintered parts. They have proposed that growth in scan speed and scan spacing escalates the percentage of shrinkage, whereas increase in thickness of layer, laser energy and built chamber temperature lead to decrease in shrinkage. Ragunath et al. [22] have deliberated the effect of SLS process parameters on shrinkage values of sintered parts using Taguchi technique. They identified that the scaling factors have linear affinity with scan length and it influences more on the shrinkage of sintered part in X direction. Hopkinson et al. [23] studied the influence of specimen height and its position, and also built direction on the dimensional accuracy of sintered aluminium particles using SLS. They observed that the sintered specimen has predominant shrinkage on Z direction compared to other directions due to the sensation termed ‘Z-growth’ whereby the unwanted powder particles are sintered beyond the down facing surface by the laser energy. Ning et al. [24] investigated the influence of various direct metal laser sintering (DMLS) process parameters on dimensional shrinkage. They observed more shrinkage and non-homogeneity due to short hatch lines. Shi et al. [25] considered the influence of polymer properties, including particle size, molecular weight, crystallization rate and the molten viscosity on the shrinkage of SLS parts. They found that the dimensional accuracy of SLS parts are mostly dependable on crystallization rate. Asiabanpour et al. [26] studied the effect of several SIS process parameters on dimensional accuracy

and surface quality of sintered polymer parts using RSM and desirability hybrid approach. They have identified that the layer thickness, sintering temperature, part bed temperature, printer feedrate and heater feedrate are the most influencing parameters on part accuracy and surface quality. The aforementioned discussions exposed that quality and performance characteristics of RP parts are reliant on numerous variables that related to process rather than material characteristics. Appropriate selection of these process variables produce superior dimensional accuracy of end-use components. The literature also reveals that, none of the researchers have attempted their investigation on the optimization of shrinkage behaviour of SIS processed high density polyethylene parts.

Therefore, in this work, an exhaustive study has been made to envisage the influence of four SIS variables such as, heater energy, printer feedrate, heater feedrate, layer thickness on the shrinkage behaviour of SIS processed HDPE parts. The experiments are designed and performed based on RSM based box-behnken design. Percentage variance in the dimensions of sintered specimens and CAD model along length, width and thickness directions are considered as responses. Desirability approach is employed in optimizing the process parameters with suitable predication models. A validation experiment is conducted to imitate the effectiveness proposed models at optimal level of process variables. The quantitative effect of these parameters on shrinkage is obtained using sensitivity analysis.

Experimental Details

Development of SIS System

SIS machine is custom built to fabricate the parts as shown in Fig. 1 and the detail description of mechanical assembly, electronic systems, controller and software modules are elaborated below.

Feed and build tanks

The feed tank is used to store and deliver the polymer powder materials to build tank through a roller mechanism. It is made of aluminium sheets with a size of 250 × 200 × 8 mm. The build tank also called as part bed constructed using aluminium sheet with size of 200 × 200 × 2 mm where in desired parts are fabricated. The upward and downward movement of both the tanks are achieved through a simple power screw mechanism which is driven using a Nema 23 stepper motor. Four round steel bars are used to guide the bed plate of both the tanks. Possible swaying of top plate as it moves vertically is eliminated with the help of linear bearing fitted at the bottom of the tanks. The movement of both feed and build tanks are devised to push the required quantity of powder in a precise way for the designated layer thickness.

Heater assembly

Ceramic heater with temperature control unit is integrated to the system to perform sintering and maximum temperature of 350 °C can be achieved. The heater unit is moved along the horizontal direction using a linear actuator and its feed rate is also controlled. A proportional, integral, derivative (PID) control algorithm is implemented to maintain the desired temperature for sintering of polymer powders. The heating element comprising of two lamps of 240 V/1000watts of each, fixed in aluminum sheet casing in the parallel direction with the spacing of 10 mm. The heater assembly is coupled with a belt and pulley drive and they are actuated through a double shaft stepper motor.

Part bed heater

After sintering process, the part bed is immediately exposed to ambient temperature which causes curling and twisting of sintered part layers. In order to avoid this issue, part bed is maintained with a specific temperature using a surface plate

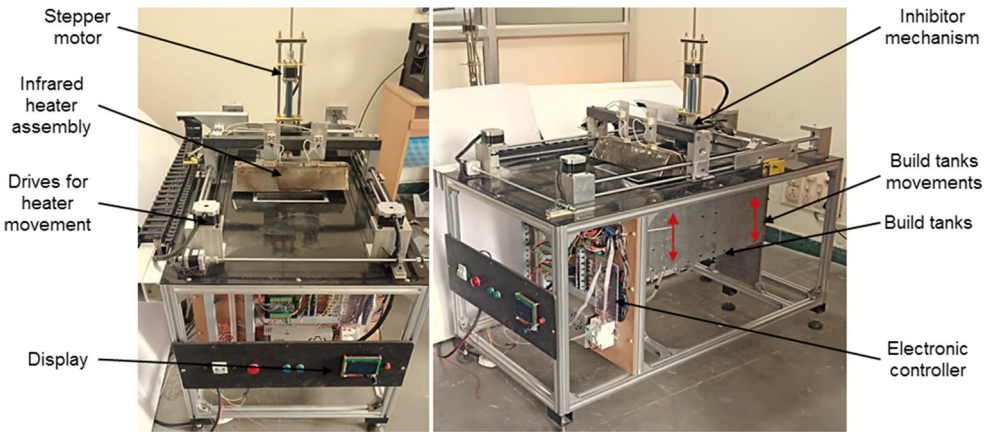

Fig. 1 Developed SIS system

heater which is attached at the bottom of build tank. The part bed is maintained to approximately 90°–100 °C to achieve uniform adhesion between first layer and powder bed.

Preparation of inhibitor and delivery mechanism

Preliminary experiments are conducted to evaluate the performance of each inhibitor through applying heat energy on the polymer powder with inhibitor at the periphery. It is observed that, barium chloride and potassium iodide (KI) are obtained uniform penetration on the powder surface than other inhibitors. However, KI has high solubility which is essential during post processing for cleaning of inhibitor without much effort. Hence, KI (133 g /100 ml of water) is mixed with water to form aqueous saturated KI solution. In addition, small amount of isopropyl alcohol (IPA) is added to avoid the formation of droplets. After many iterations, the proportion of KI, H_2O and IPA is found to be 50 g: 42.5 ml: 8 ml to perform inhibition at the part boundary. Delivery mechanism consists of a syringe which is driven using a stepper motor in turn connected to a linear screw. A nozzle of 0.5 mm diameter is attached at the tip of syringe which can store 60 ml of inhibitor solution. The complete setup is coupled with roller mechanism so that both the motions are synchronized appropriately.

Sensors, actuators and controller

The SIS system consists of five independent movements such as translation along X, Y, Z, deposition of inhibitor and travel of heater. The XY planar motion is achieved through a timing belt and pinion setup actuated using a stepper motor. The up and down motion of feed and build tanks along Z direction is actuated through a stepper motor in such a way that, desired layer thickness is maintained for sintering of polymer powders. When the feed tank is moved upward direction of 0.1 mm then simultaneously build tank is moved downwards of same thickness. These two motions are coupled in a routine way so as to make the parts with desired layer thickness is obtained. As per the desired part profile, numerical control (NC) tool path is generated which enables to deliver the inhibitors at the part boundaries. After deposition of inhibitors, heater assembly is moved along the XY plane and desired temperature is accomplished using a PID controller. ATMEGA 2560 arduino based controller with Ramps 1.4 board is used to control all five motions of SIS system. SMPS (switched mode power supply) is connected with the controller which will supply the power of 5 V. The limit switches are placed in X, Y, and Z directions and hence motions are restricted to 230 mm, 470 mm and 200 mm respectively. Two thermistors are used to measure the temperature of heater and bed heater which forms a closed loop control system and temperature is monitored in LCD. The two solid state relays are used to switch heater and control the temperature appropriately.

Materials and Measurements

The desired three dimensional (3D) CATIA models are exported as a stereolithograpic (.stl) file. The STL file is imported into *Slic3r* software which slices the STL file with specific layer thickness and then it is transformed into G-codes. These G-Codes, then, are imported into *Pronterface* software to create machine tool paths of SIS machine for smearing the inhibitor at the part boundary. As per the machine path generation, HDPE powder is deposited with a desired layer thickness from the storage chamber using a roller mechanism. Inhibition is carried out with reference to required part profile which act as support material for the part. Sintering phenomenon is achieved through controlling the temperature of ceramic heater with appropriate feed rate. The layer-by-layer deposition of powder, inhibition, and sintering is performed until the required part is fabricated. Post processing of cleaning of inhibitor from the built part completes the SIS process.

Investigation of diverse SIS parameters such as thickness of powder layer, feed rate of heater, inhibition printer rate and heater energy are considered for the experimental studies. Their ranges are selected (Table 1) based on exhaustive pilot experimentation and literature studies. During experimentation, build tank temperature, printer nozzle diameter and nozzle stand-off distance are assigned constant values as 90 °C, 0.5 mm and 5 mm respectively.

High density polyethylene (HDPE) material with an average grain size ranging of 35–80 μm supplied by JP Polymers, India is utilized for part fabrication. During the course of experiments, 100% virgin powder is used to avoid irregularities in sintered parts. Figure 2 shows the shape and size (135 × 35 × 8 mm) of the SIS test specimen used to investigate the shrinkage. The shrinkage measurement is made in the specimen along the length (L), width (W) and thickness (T) and their mean value is accounted. The dimensions are measured using Checkmaster (Model: 216–242, Helmel.Inc., USA) bench top co-ordinate measuring machine equipped with Geomet® 7.00.035

Table 1 SIS process parameters and their levels

Parameters	Unit	Symbol	Levels		
			Low	Medium	High
Layer thickness	mm	A	0.1	0.2	0.3
Heater energy	J/mm^2	B	22.16	25.32	28.48
Heater feedrate	mm/s	C	3	3.5	4
Printer feedrate	mm/min	D	80	100	120

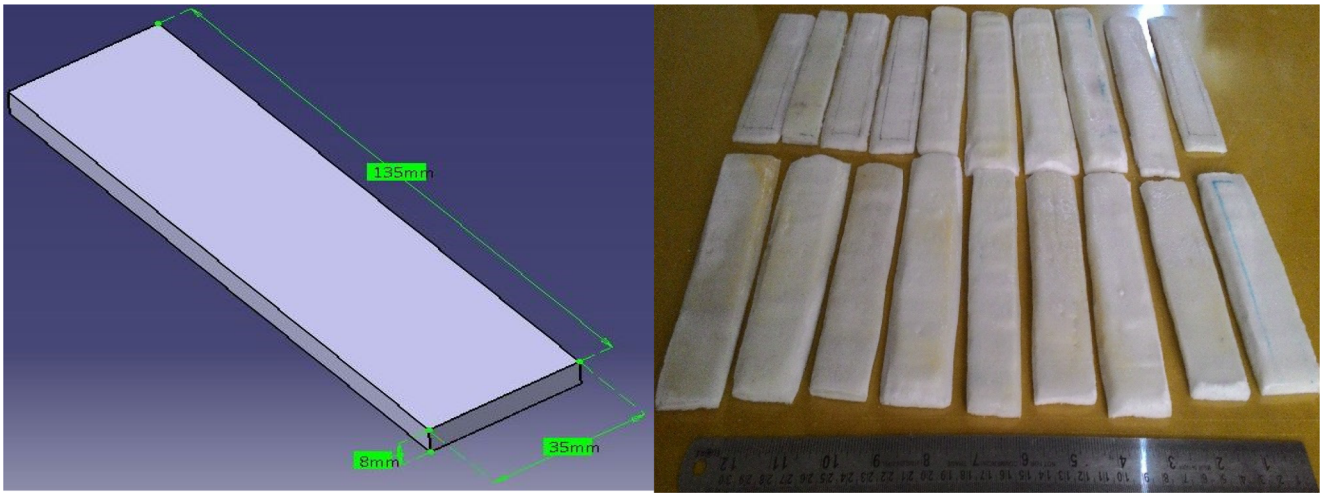

Fig. 2 Specimen with dimensions; sample fabricated specimen

universal CMM software, having measuring range of 400 × 500 × 350 mm as shown in Fig. 3. The experimental design matrix and measured shrinkage values are presented in Table 2. It is observed from table that the measured values at the length and width are comparatively higher than the dimension of CAD model at all the circumstances. These variations in dimension can induce stresses in the specimens and hence it has to be minimized. Based on measured dimensions, shrinkage of a specimen is calculated by following,

$$\%dX = \frac{|X - X_{CAD}|}{X_{CAD}} \times 100 \quad (1)$$

where X_{CAD} represent the dimension from CAD model, X is the actual size measured using Vernier calliper and $\%dX$ stands for percentage change in dimension along specified direction.

Fig. 3 Measurement of test specimen dimensions using co-ordinate measuring machine with Geomet software

Experimental Design

Execution of experiments with appropriate planning to achieve desired efficiency is essential. The present study incorporates RSM, a collection of mathematical methods, experimental strategies and statistical inferences to analyse and optimize the response values obtained through experimentation [27]. In this work, dimensional accuracy is considered to be a response variable, because it influences the particle size, shape, packing direction and density. However, evaluation of shrinkage with respect to various SIS process variables such as thickness of built layer (A), heat energy (B), feed rate of heater (C), and printer feed rate (D) is of great importance to obtain dimensional stability of sintered parts.

The range of SIS parameters is decided on the basis of polymer properties and conducting several pilot experiments. From the pilot studies, it is observed that the sintering does not ascend if the heater input energy is below 22.16 J/mm^2 and polymer powder particles confiscations to degradation further than 28.48 J/mm^2. The built chamber is preheated to 85 °C to overcome thermal distortion and avoid sticking of sintered polymer particles with recoater. Increasing built chamber temperature above 85 °C increases the curing time of the polymer particles that resulted in more crystallinity of polymer structure. Levels of heater feedrate and printer feedrate are suitably selected by changing one variable at a time. All other parameters associated to SIS process are kept constant throughout the experimentation. This present study, Box-behnken design (BBD) based on RSM [28] is employed to outline the experiments. Generally, BBD is used for performing non-sequential experiments and no axial points are considered which confirms that all design points

Table 2 Experimental design matrix and collected data

S.No	Layer thickness (mm)	Heater energy (J/mm^2)	Heater feedrate (mm/s)	Printer feedrate (mm/min)	Shrinkage of the specimen			
					Length (mm)	Width (mm)	Thickness (mm)	Avg. Shrinkage (S) (mm)
1	0.3	25.32	4.0	100	9.3423	4.2529	2.1179	5.2377
2	0.2	28.48	3.0	100	10.2303	4.5581	1.6762	5.4883
3	0.1	25.32	4.0	100	17.0400	3.6354	2.4169	7.6974
4	0.2	25.32	3.5	100	12.5661	3.8905	−1.8663	4.8634
5	0.3	25.32	3.5	80	11.1515	3.5519	2.3185	5.674
6	0.1	25.32	3.5	120	10.5594	4.0534	−2.4621	4.0502
7	0.2	25.32	4.0	120	15.6583	3.9839	2.3252	7.3224
8	0.2	25.32	3.0	120	10.4607	3.8086	−1.7165	4.1842
9	0.2	28.48	4.0	100	10.7240	3.5946	1.9197	5.4127
10	0.2	25.32	3.5	100	12.5332	4.3263	−1.8715	4.9960
11	0.2	28.48	3.5	80	11.6775	4.4485	−1.7492	4.7922
12	0.2	22.16	3.5	80	12.3357	3.5171	−1.9155	4.6457
13	0.3	25.32	3.0	100	15.9083	4.0103	2.1407	7.6864
14	0.2	22.16	3.5	120	10.0990	5.3879	−1.8748	4.5373
15	0.2	22.16	4.0	100	13.1253	4.1959	1.9084	6.4098
16	0.3	22.16	3.5	100	7.9935	5.2615	1.6102	4.9551
17	0.2	25.32	3.5	100	11.2174	4.2203	−1.8469	4.5302
18	0.1	25.32	3.0	100	8.5856	5.1642	−2.1084	3.8804
19	0.2	25.32	4.0	80	14.7044	2.7470	−1.8574	5.1980
20	0.2	25.32	3.5	100	11.1186	3.9451	−1.8413	4.4074
21	0.2	25.32	3.5	100	11.0202	3.9024	−1.8590	4.3545
22	0.2	25.32	3.0	80	14.8032	4.5840	2.1377	7.1749
23	0.2	28.48	3.5	120	10.1319	3.4132	−1.8365	3.9028
24	0.1	25.32	3.5	80	13.3557	4.3630	−2.0546	5.2213
25	0.1	28.48	3.5	100	7.9277	5.0008	−1.6300	3.7661
26	0.1	22.16	3.5	100	12.0398	5.3533	−2.5373	4.9519
27	0.3	28.48	3.5	100	9.6714	4.2712	2.3341	5.4256
28	0.2	22.16	3.0	100	9.4081	5.1495	1.8693	5.4756
29	0.3	25.32	3.5	120	10.9082	4.0031	−2.5834	4.9536

plunge within the safe range of operational parameters [29]. A total of twenty-nine experiments including five central points per block are conducted based on the design matrix of three-level four-factors shown in Table 1, using Design Expert 7 statistical software. The following second-order polynomial equation gives the relation between predictor and dependent variables,

$$Y = C_0 + \sum_{i=1}^{n} C_i X_n + \sum_{i=1}^{n} d_i {X_i}^2 \pm \varepsilon \quad (2)$$

The empirical models are developed by accumulating the necessary data from design of experiments, followed by the statistical multiple regression technique. Further, ANOVA is adopted to rationalize the significance of the developed regression models.

Analysis and Discussions

Development Shrinkage Models Using Statistical Analysis

Based upon BBD, experiments are planned and conducted, as shown in Table 2. They are conducted rigorously and corresponding test specimens are fabricated. The degree of sensitivity of the analysis with respect to various factors that influence the responses and interactions between the existing factors are examined. ANOVA is employed to evaluate these aspects where in robustness of the developed models are tested. Table 2 shows the inference on dimensional shrinkage of proposed mathematical model using ANOVA. The models are developed at 95% confidence interval and the results of linear, interaction and quadratic models are given in Table 3. The multiple regression co-

efficient (R^2) for developed models are obtained close to unity, which indicates better coherence of response model and actual data [30]. The developed models provided higher values of determination co-efficient and adequate precision which are obtained as: $R^2 = 0.9827$ and AP = 27.514 for shrinkage. Hence, the models have high integrity of fit and they can provide satisfactory prediction of experimental results.

In addition to ANOVA, normal probability plot and predicted vs actual plots for dimensional shrinkage is also presented in Fig. 4(a-b) to verify normality assumptions. It is observed that, the residuals fall on a straight line which specifies that error is normally dispersed and they have no noticeable pattern and unfamiliar structure supporting that the terms mentioned in the developed models are significant.

From the developed models, few terms may be regarded as insignificant terms due to their "Prob. > F" value being more than 0.050. These insignificant terms might be discarded through backward eliminate selection method and significant terms are retained for further analysis. The established quadratic shrinkage model is given as,

$$Avg.Shrinkage(S) = 65.614 + 62.988A + 1.461B - 36.791C - 0.425D + 1.31AB - 31.329AC - 0.159BC + 0.128CD + 28.716A^2 - 0.018B^2 + 4.983C^2 + 0.0001D^2 \quad (3)$$

Individual Effect of Process Variables on Shrinkage

In this contemporary study, the influence of different SIS process variables such as heater energy and feedrate, layer thickness, and printer feedrate on shrinkage of various specimens are experimentally investigated. From Fig. 5(a-d), it is evident that the selected process parameters have a substantial influence on shrinkage.

Influence of layer thickness

Increase in the thickness of layer from 0.1 mm to 0.3 mm resulted in increase of shrinkage, as observed in Fig. 5(a). It is because of the smaller layer thickness results in more overlapping zone of melting and repetition of heating and cooling cycles to the previous sintered layers diminishes the heat exposed surface and hence shrinkage is abridged. Further increase in layer thickness leads to poor storing of polymer particles in the part built chamber and the tendency of curl in the powder layers which adhered with roller restricts subsequent layer from appropriate sintering resulting poor shrinkage beside the part built direction [17].

Table 3 ANOVA and adequacy of the quadratic model for average shrinkage

Source	Sum of squares	DOF	Mean square	F-Value	Prob > F	
Model	33.05	14	2.361	56.828	0.0001	Significant
A	1.58	1	1.587	38.214	0.0001	Significant
B	0.39	1	0.398	9.598	0.0079	Significant
C	0.95	1	0.956	23.023	0.0003	Significant
D	1.17	1	1.175	28.287	0.0001	Significant
AB	0.68	1	0.685	16.505	0.0012	Significant
AC	9.81	1	9.814	236.207	0.0001	Significant
AD	0.05	1	0.050	1.222	0.2876	Not significant
BC	0.25	1	0.254	6.135	0.0266	Significant
BD	0.15	1	0.152	3.669	0.0761	Not significant
CD	6.54	1	6.541	157.421	0.0001	Significant
A^2	0.53	1	0.534	12.873	0.003	Significant
B^2	0.2	1	0.209	5.052	0.0412	Significant
C^2	10.06	1	10.065	242.233	0.0001	Significant
D^2	0.02	1	0.020	0.503	0.4897	Not significant
Residual	0.58	14	0.041			
Lack of fit	0.25	10	0.025	0.318	0.9352	Not significant
Pure error	0.32	4	0.080			
Cor. Total	33.63	28				
Std. Dev.		0.2		R^2		0.9827
Mean		5.21		Adj.R^2		0.9654
C.V.		3.91		Pred. R^2		0.9408
PRESS		1.99		Adeq. Precision		27.514

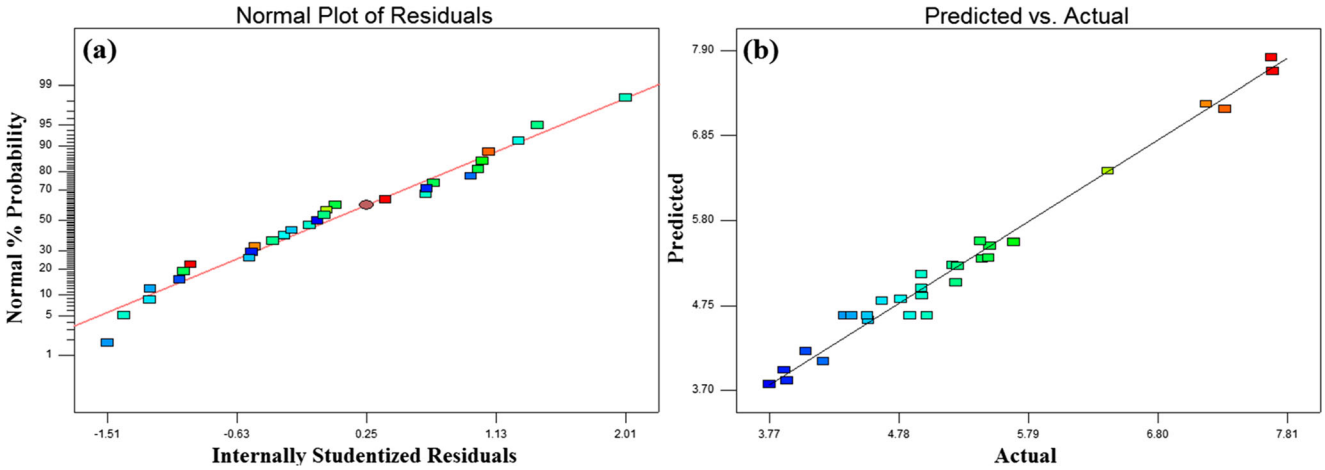

Fig. 4 Normal probability plot of residuals for average shrinkage, (**b**) Plot of predicted vs actual response for average shrinkage

Influence of heater energy

The heat energy applied on the polymer powder is increased from 22.16 J/mm^2 to 28.48 J/mm^2 and its effect on shrinkage is evaluated. The range of heater energy have been chosen on basis of melting point of HDPE. From the Fig. 5(b), it has been perceived that there is decrease in shrinkage as the heater energy is amplified from 22.16 J/mm^2 to 28.48 J/mm^2. Increase in heater energy origins growth in width and depth of heater energy penetration. Consequently, the dimensions of sintered specimen slightly increased and achieved desired dimensions after curing. The growth of heater energy also upsurge the curing area temperature which leads to decline in amount of crystallinity [22, 31, 32] of the structure and

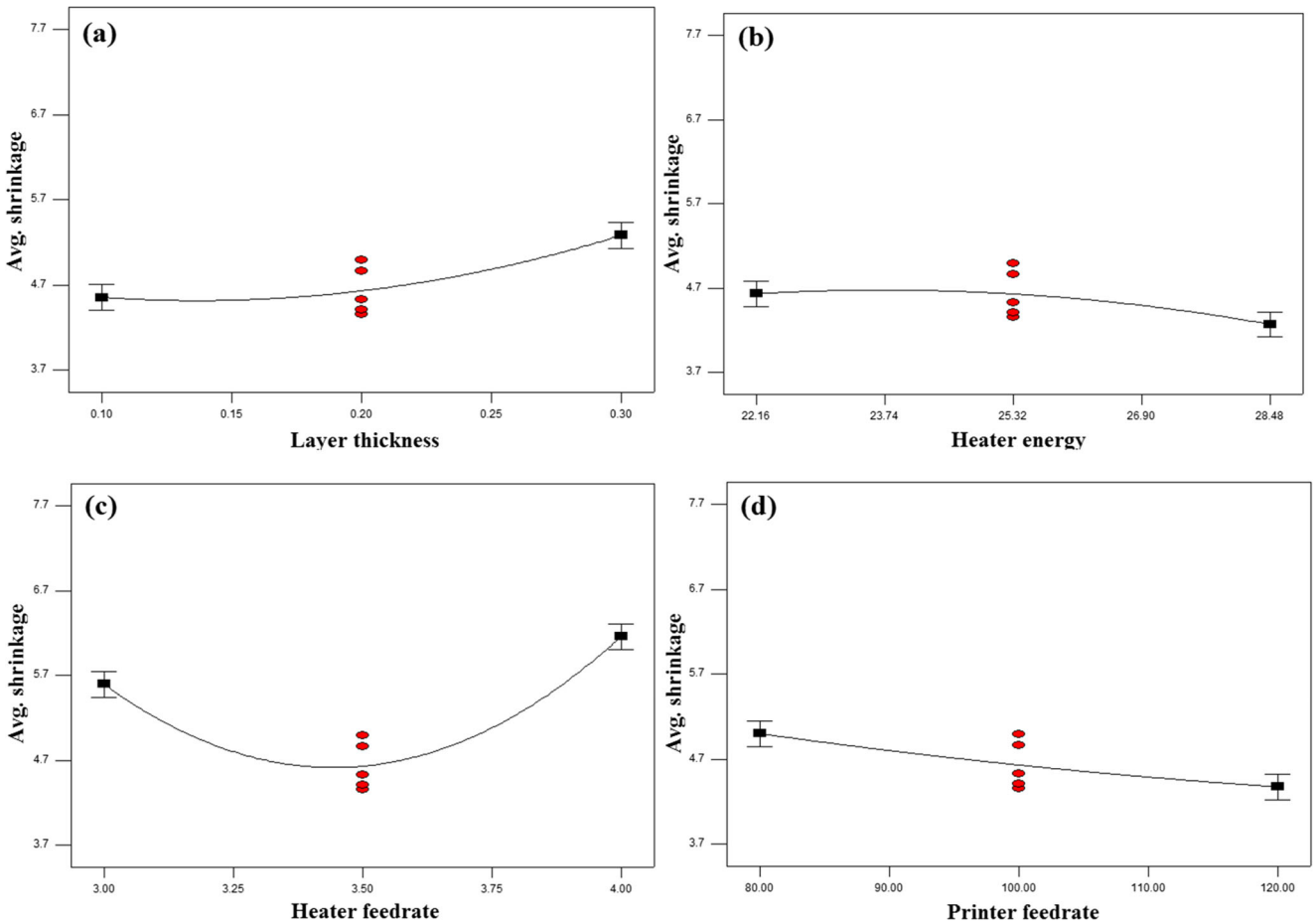

Fig. 5 Effect on Average shrinkage for different parameters: (**a**) layer thickness, (**b**) heater energy, (**c**) heater feedrate, and (**d**) printer feedrate

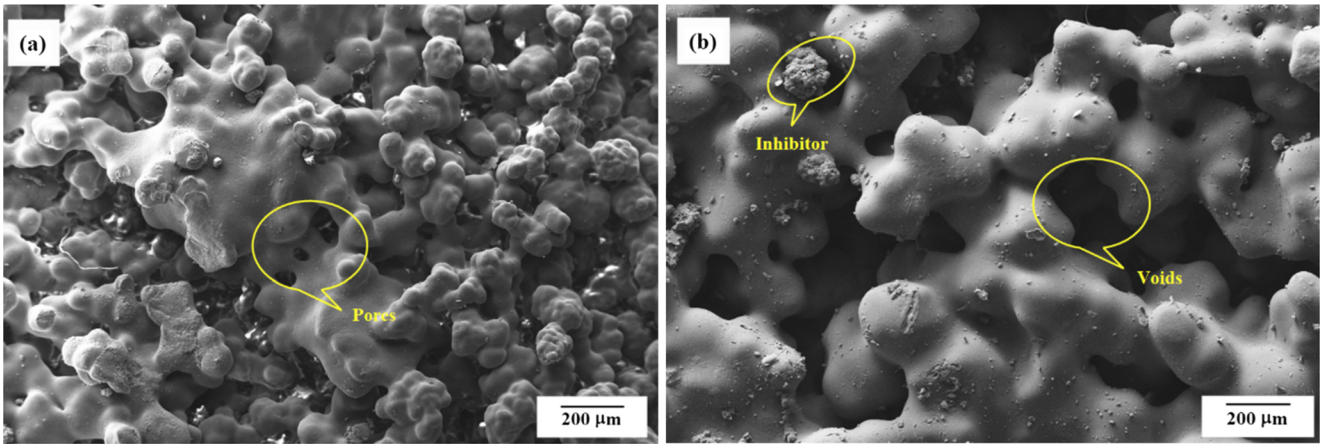

Fig. 6 Microstructure of sintered specimen at heater energy of 22.16 J/mm^2 and 28.48 J/mm^2

diminishes the formation of voids and pores. Reduction in crystallinity causes reduction in shrinkage. The same trend has also been found for selective laser sintering process [19] when glass filled polyamide is used. Further, the microstructure of sintered specimen with different input heater energy is depicted in Fig. 6(a-b). Better coalescence of polymer particles are observed at heater energy of 28.16 J/mm^2 in comparison to 22.16 J/mm^2 and thereby dimensional accuracy improved at higher heater energy.

Influence of heater feedrate

The shrinkage is decreased with an escalation of feedrate of heater from 3 mm/s to 3.5 mm/s and further rise of heater feed rate increases shrinkage as shown in Fig. 5(c). At greater feedrate of heater, the energy absorption of polymer particles regimes has shorter exposure resulted in non-uniform sintering and weak bonding of particles. Hence, each layer tends to curl and cling with rollers causes improper sintering of subsequent layers. On the contrary, lower heater feedrate increases the contact time between heater and powder bed. Thus, sufficient heat energy is supplied over the powder surface and the temperature fields tends to be uniform, resulting in formation of compact structure with less shrinkage. The same trend can be seen in the SLS process [19]. However, very low heater feedrate may cause over melting of powder particles which reduces the forming efficiency and hence shrinkage increases.

Influence of printer feedrate

Effect of printer feedrate on shrinkage can be seen in Fig. 5(d). The increase in printer feedrate from an inferior level (80 mm/min) to a higher level (120 mm/min) causes decrease in shrinkage. It may be because of the fact that at lower printer feedrate, inhibition spell increases and the inhibitor penetrates apart from the actually targeted regions. This excess inhibitor penetration leads to prevent powder from effective sintering. Hence, shrinkage increases due to inappropriate sintering of polymer powders. However, increasing of printer feedrate offers precise inhibition on selected area, resulting inferior shrinkage. Moreover, deposition of inhibition depends on geometrical complexity and thickness of each layer.

Interaction Influence of Process Variables on Shrinkage

The interaction between the process variables on shrinkage characteristics of sintered parts are described by three-dimensional surface plots as shown in Fig. 7(a-c). It is observed that shrinkage decreases from 4.1 mm to 3.7 mm with increase in heater energy and layer thickness. However, the specimens fabricated at a high level of heater energy (28.48 J/mm^2) and low level of layer thickness (0.1 mm) have less part shrinkage. It is due to the fact that at high heater energy and minimal layer thickness, the transfer of heat energy to part bed is appropriate for better fusion of particles to produce dense structure, resulting in lesser shrinkage.

Figure 7(b) shows the interaction effect of thickness and feedrate of heater on dimensional shrinkage. It is seen that specimens fabricated at low heater feedrate (3 mm/s) and low layer thickness (0.1 mm) yield less shrinkage of 3.68 mm. However, increase in feedrate of heater from low to high level drastically increases the shrinkage. It may be attributed due to the fact that higher heater feedrate provides deficient heat energy to the polymer particles at unit time for a unit area that causes improper sintering, resulting increase in crystallinity which leads to higher shrinkage.

Figure 7(c) demonstrates the interaction effect on thickness of layer and feed rate of printer on shrinkage. It is observed that, shrinkage reduces with the increase in feedrate of printer from low to high level. Specimen fabricated with high printer feedrate (120 mm/min) and low layer thickness (0.1 mm) has attained less shrinkage. It is due to the fact that low printer

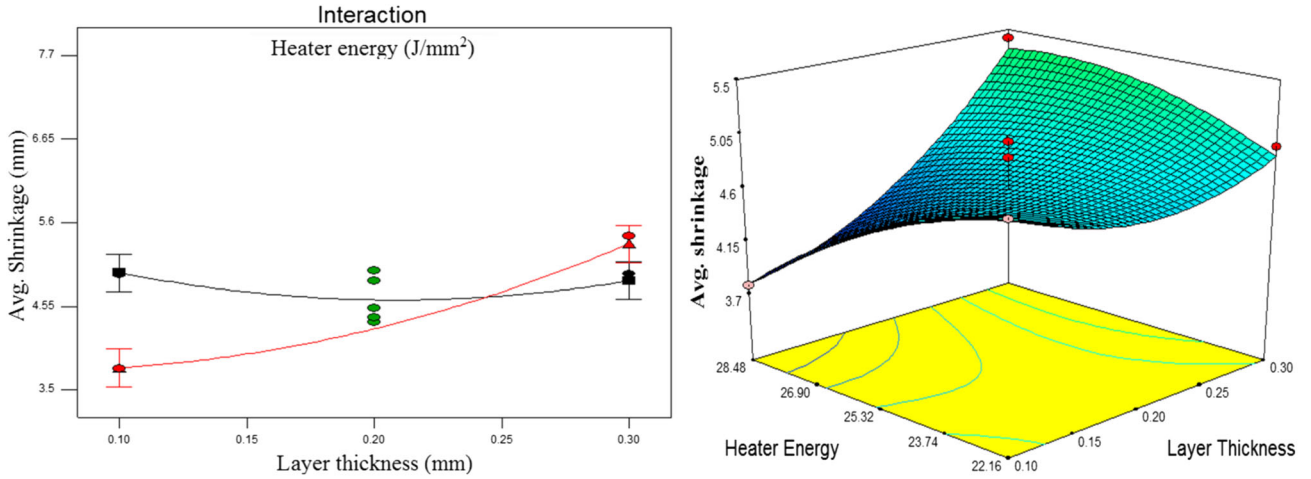

(a)

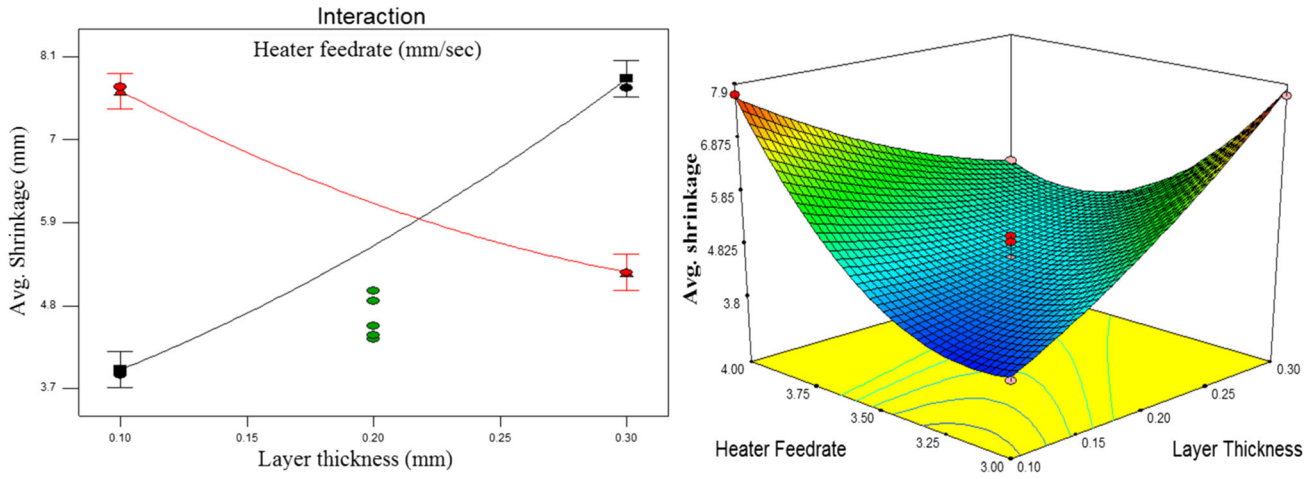

(b)

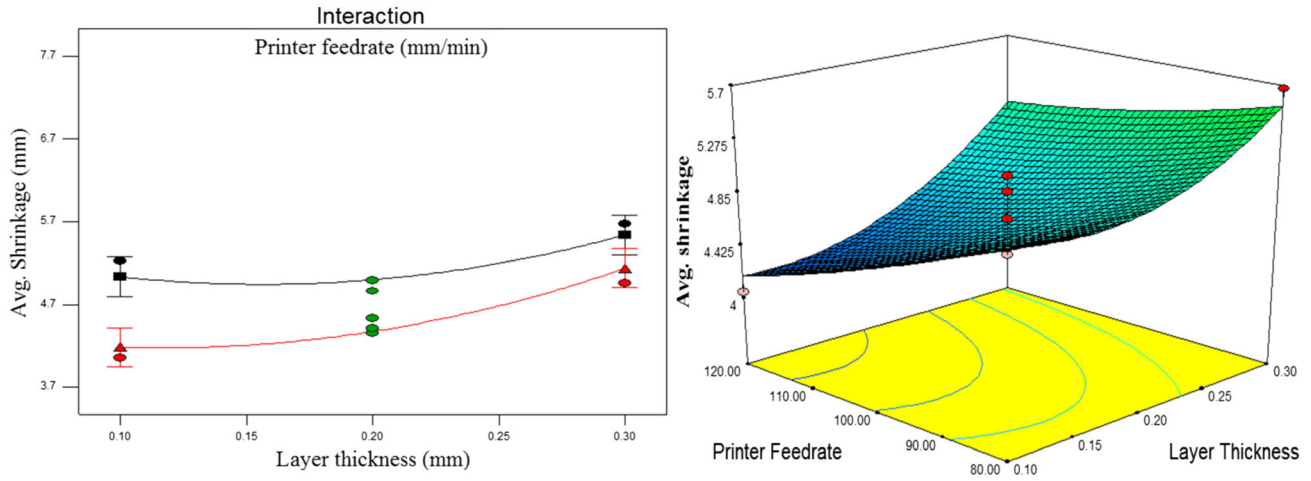

(c)

Fig. 7 Three dimensional response surface plots on average shrinkage for different parameters: (**a**) layer thickness and heater energy, (**b**) layer thickness and heater feedrate, and (**c**) layer thickness and printer feedrate

feedrate increases the extent of printing time on part boundary. The excess printing of inhibitor will penetrate away from the actually targeted region that causes irregular layer sintering and thereby increase in shrinkage of part body and its boundary.

Optimization

Optimization was carried out to identify the optimal SIS parameters to obtain minimal shrinkage in sintered specimen. RSM based desirability optimization approach [33] is used. In this strategy, the goal used for the average shrinkage is 'minimize' and for the factors is 'within range'. In addition, weights are assigned for each response ranging from 0.1 to 10 to fine-tune the contour of its desirability function. The significance of process variables is varied from the least to most desirable (i.e., 1 and 5). From the desirability-based approach, varied best solutions are obtained and highest desirability solution is preferred. The best optimized conditions are obtained at desirability of 1.00 for average shrinkage of 3.677 mm, are heater energy of 27.80 J/mm^2, layer thickness of 0.12 mm, feedrate of heater 3.39 mm/s, and feedrate of printer 102.63 mm/min respectively as shown in desirability ramp function (Fig. 8) In the desirability ramp function, the dot of each ramp denotes the reflection of parameter setting and the height of the dot indicates the amount of desirability [34]. A validation experiment is conducted to confirm the effectiveness of developed models. The optimal level of process parameters attained through desirability optimization technique is used to conduct the validation experiment. Table 4 shows the comparison of shrinkage values obtained through confirmation experiment and desirability approach. The confirmation experiment results shows better closeness between the predicted and actual values with an average error of 3.081% and hence the established model is suitable for estimating the shrinkage characteristics of parts made using SIS process.

Sensitivity Analysis

Sensitivity analysis is performed to ascertain the qualitative and quantitative effectiveness of process variables and rank them by their order of prominence. It has remarkable importance in validating of model where in efforts are attempted to associate the deliberated output to the distinguished data [35]. Hence, it plays a vital role in identifying the input process variables by applying the greatest impact on the model outputs. Sensitivity with reference to a design parameter is derived from the partial derivative of the function under consideration to the corresponding process parameters [36].

The insistence of the present study is to predict the tendency of dimensional shrinkage with reference to diverse SIS process variables such as feedrate of heater, thickness of each layer, heater energy, and feedrate of printer. The shrinkage sensitivity equations are obtained by partially differentiating the (equation (1)) with respect to A, B, C and D. The following equations (equations (4–7)) represents the shrinkage sensitivity for the SIS variables which is given by,

$$\frac{\partial S}{\partial A} = 62.988 + 1.31B - 31.329C + 57.432A \tag{4}$$

$$\frac{\partial S}{\partial B} = 1.461 + 1.31A - 0.159C - 0.036B \tag{5}$$

$$\frac{\partial S}{\partial C} = -36.791 - 31.329A + 0.128D + 9.966C \tag{6}$$

$$\frac{\partial S}{\partial D} = -0.425 + 0.128C + 0.0002D \tag{7}$$

If the shrinkage sensitivity of certain process variable is positive implies that, an augmentation in the shrinkage due to a growth in design variables [37].

The sensitivities of these SIS process variables on shrinkage are presented in Fig. 9(a-d) by solid bars with respect to various processing conditions as premeditated using BBD in Table 2. These results revealed that, the layer thickness and heater

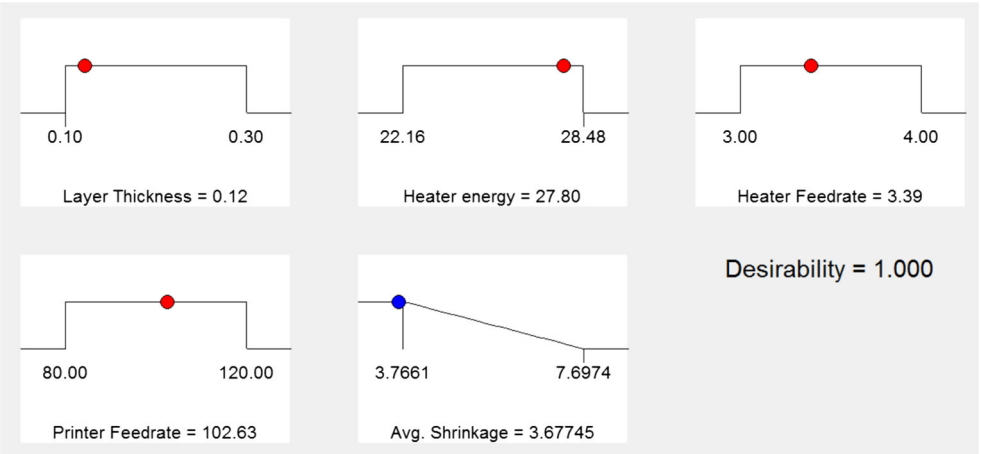

Fig. 8 Desirability ramp function for numerical optimization

Table 4 Comparison of shrinkage predicted by conformation experiment and desirability

Layer thickness (mm)	Heater energy (J/mm^2)	Heater feedrate (mm/s)	Printer feedrate (mm/min)	Average shrinkage (mm)		Error %
				Predicted	Actual	
0.12	27.8	3.39	102.63	3.677	3.792	3.021

feedrate are more sensitive on shrinkage than heater energy and printer feedrate. It means that a small variation of layer thickness and heater feedrate causes large changes in shrinkage. Therefore, the results presented in Fig. 9(a-d) discloses that layer thickness has a great influence on shrinkage, followed by heater feedrate, heater energy and printer feedrate.

Conclusions

Parametric and optimization studies are conducted on evaluation of shrinkage characteristics of SIS part specimens made through HDPE. Experimental investigations and ANOVA analysis on selected SIS process variables revealed

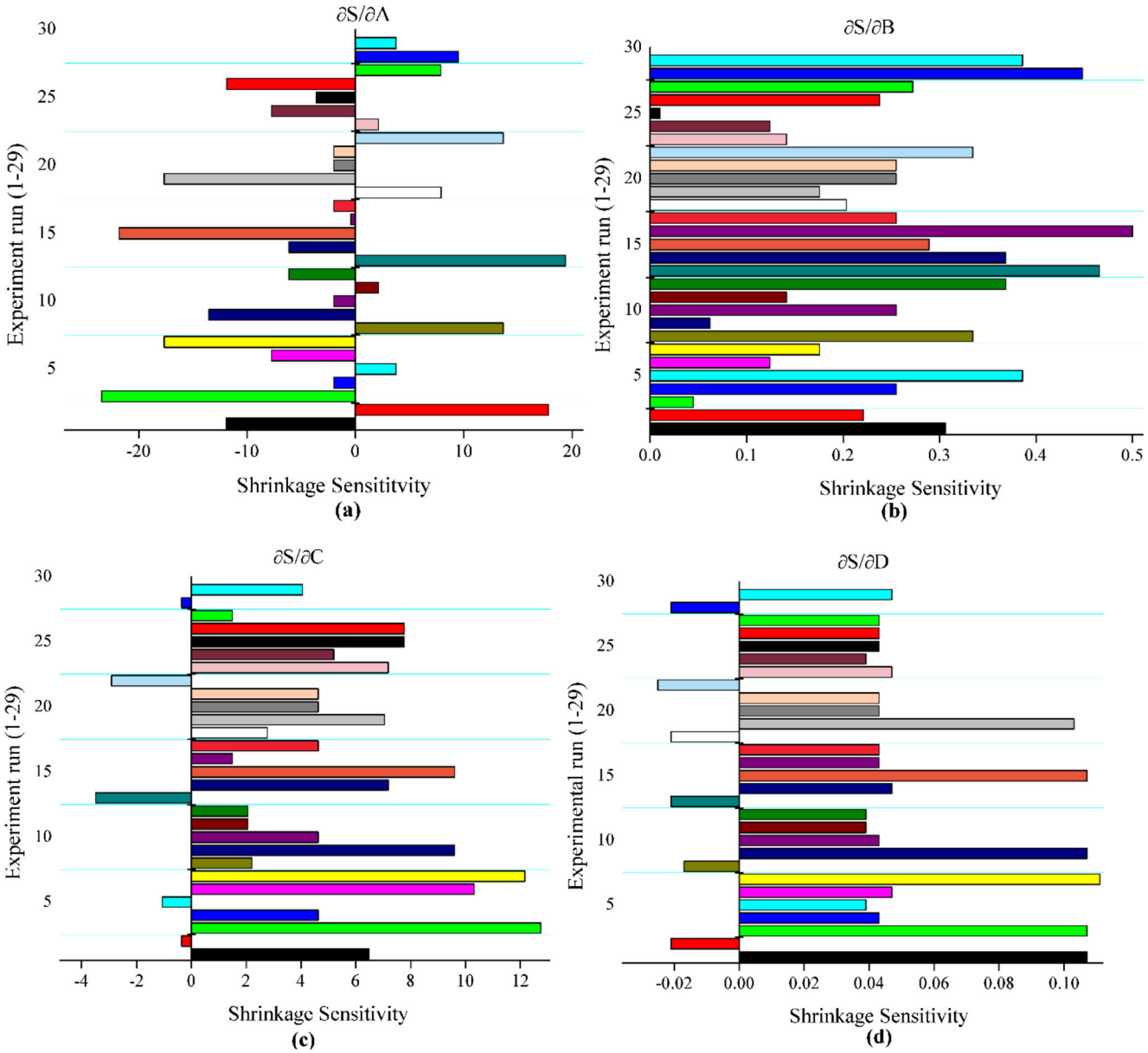

Fig. 9 Shrinkage sensitivity of layer thickness, heater energy, heater feedrate and printer feedrate

the effect on shrinkage. It is observed that, the thickness of polymer powder layer has predominantly influence the shrinkage of specimens in comparison with other SIS process variables. The dimensional accuracy of sintered part increases directly proportional to the heater energy and feedrate of printer, whereas increase in layer thickness and feedrate of heater increases the shrinkage of SIS built part. Improved dimensional accuracy of SIS built are found to be with lower thickness of built layer (0.12 mm), higher heater energy (27.80 J/mm^2), average feedrate of heater (3.39 mm/s) and medium feedrate of printer (102.63 mm/min). The results of confirmation experiment agree well with the predicted optimal values with an acceptable error of 3.02%. Sensitivity analysis revealed that the variation in layer thickness, heater feedrate and heater energy are more sensitive to shrinkage, whereas printer feedrate has insignificant effect.

Acknowledgements The funding support from Armament Research Board (ARMREB), Defence Research and Development Organization (DRDO), Government of India is thankfully acknowledged. (ARMREB/MAA/2015/167).

References

1. ASTM F2792-12a (2012) Standard terminology for additive manufacturing technologies (withdrawn 2015). ASTM International, West Conshohocken
2. Pham DT, Demov SS (2001) Rapid manufacturing: the technologies and applications of rapid prototyping and rapid tooling. Springer-Verlag, London
3. Chua CK, Leong KF (1998) Rapid prototyping: principles and applications in manufacturing. John Wiley and Sons Inc., Singapore
4. Chua CK, Leong KF, Lim CS (2003) Rapid prototyping: principles and applications. World Scientific, Singapore
5. Averyanova M, Cicala E, Bertrand PH, Grevey G (2012) Experimental design approach to optimize selective laser melting of martensitic 17-4 PH powder: part I – single laser tracks and first layer. Rapid Prototyp J 18(1):28–37
6. Bikas H, Stavropoulos P, Chryssolouris G (2016) Additive manufacturing methods and modelling approaches: a critical review. Int J Adv Manuf Technol 83:389–405
7. Khoshnevis B, Asiabanpour B, Mojdeh M, Palmer K (2003) SIS – a new SFF method based on powder sintering. Rapid Prototyp J 9(1):30–36
8. Khoshnevis B, Yoozbashizadeh M, Chen Y (2012) Metallic part fabrication using selective inhibition sintering (SIS). Rapid Prototyp J 18(2):144–153
9. Rosochowski A, Matuszak A (2000) Rapid tooling- the state of art. J Mater Process Technol 106(1–3):191–198
10. Mahapatra SS, Sood AK (2012) Bayesian regularization-based Levenberg–Marquardt neural model combined with BFOA for improving surface finish of FDM processed part. Int J Adv Manuf Technol 60:1223–1235
11. Sachdeva A, Singh S, Sharma VS (2013) Investigating surface roughness of parts produced by SLS process. Int J Adv Manuf Technol 64:1505–1516
12. Sood AK, Ohdar RK, Mahapatra SS (2012) Experimental investigation and empirical modelling of FDM process for compressive strength improvement. J Adv Res 3:81–90
13. Rayegani F, Onwubolu GC (2014) Fused deposition modelling (FDM) process parameter prediction and optimization using group method for data handling (GMDH) and differential evolution (DE). Int J Adv Manuf Technol 73:509–519
14. Rajamani D, Esakki B (2017) Examining mechanical strength characteristics of selective inhibition sintered HDPE specimens using RSM and desirability approach. IOP Conf Ser: Mater Sci Eng 234: 012002
15. Esakki B, Rajamani D, Arunkumar P (2017) Modeling and prediction of optimal process parameters in wear behaviour of selective inhibition sintered high density polyethylene parts. Prog Addit Manuf. https://doi.org/10.1007/s40964-017-0033-z
16. Karapatis NP, Van Griethuysen JPS, Glardon R (1998) Direct rapid tooling: a review of current research. Rapid Prototyp J 4(2):77–89
17. Singh S, Sharma VS, Sachdeva A (2012) Optimization and analysis of shrinkage in selective laser sintered polyamide parts. Mater Manuf Process 27:707–714
18. Sood AK, Ohdar RK, Mahapatra SS (2009) Improving dimensional accuracy of fused deposition modelling processed part using grey Taguchi method. Mater Des 30:4243–4252
19. Negi S, Sharma RK (2016) Study on shrinkage behaviour of laser sintered PA 3200GF specimens using RSM and ANN. Rapid Prototyp J 22(4):645–659
20. Senthilkumaran K, Pandey PM, Rao PVM (2009) Influence of building strategies on the accuracy of parts in selective laser sintering. Mater Des 30:2946–2954
21. Wang RJ, Wang L, Zhao L, Liu Z (2007) Influence of process parameters on part shrinkage in SLS. Int J Adv Manuf Technol 33:498–504
22. Raghunath N, Pandey PM (2007) Improving accuracy through shrinkage modeling by using taguchi method in selective laser sintering. Int J Mach Tool Manu 47(6):985–995
23. Hopkinson N, Sercombe TB (2008) Process repeatability and sources of error in indirect SLS of aluminium. Rapid Prototyp J 14(2):108–113
24. Ning Y, Wong YS, Fuh JYH, Loh HT (2006) An approach to minimize build errors in direct metal laser sintering. IEEE T Autom Sci Eng 3(1):73–80
25. Shi Y, Li Z, Huang S, Zeng F (2004) Effects of the properties of the polymer materials on the quality of selective laser sintering. Proc Inst Mech Eng Pt L J Mater Des Appl 218(3):247–252
26. Asiabanpour B, Khoshnevis B, Palmer K (2006) Advancements in the selective inhibition sintering process development. Virtual Phys Prototyp 1(1):43–52
27. Joseph J, Muthukumaran S (2017) Optimization of activated TIG welding parameters for improving weld joint strength of AISI 4135 PM steel by genetic algorithm and simulated annealing. Int J Adv Manuf Technol 93(1–4):23–34
28. Myers RH, Montgomery DC (1995) Response surface methodology: process and product optimization using designed experiments. John Wiley & Sons, Inc., New York
29. Box GEP, Behnken DW (1960) Some new three level designs for the study of quantitative variables. Technometrics 2:455–475
30. Rajmohan T, Palanikumar K (2013) Modeling and analysis of performances in drilling hybrid metal matrix composites using D-optimal design. Int J Adv Manuf Technol 64:1249–1261
31. Ogorkiewicz RM (1970) Engineering properties of thermoplastics. Wiley & Sons Ltd.
32. Childs THC, Tontowi AE (2001) Selective laser sintering of a crystalline and a glass-filled crystalline polymer: experiments and simulations. P I Mech Eng B J Eng Manuf 215:1481–1495

33. Derringer G, Suich R (1980) Simultaneous optimization of several response variables. J Qual Technol 12:214–219
34. Tamilarasan A, Rajamani D (2017) Multi-response optimization of Nd: YAG laser cutting parameters of Ti-6Al-4V superalloy sheet. J Mech Sci Technol 31(2):813–821
35. Kim IS, Son KJ, Yang YS, Yaragada PKDV (2003) Sensitivity analysis for process parameters in GMA welding processes using a factorial design method. Int J Mach Tool Manu 43(8):763–769
36. Lakshminarayanan AK, Balasubramanian V (2009) Comparison of RSM with ANN in predicting tensile strength of friction stir welded AA7039 aluminium alloy joints. T Nonferr Metal Soc 19(1):9–18
37. Joardar H, Das NS, Sutradhar G, Singh S (2014) Application of response surface methodology for determining cutting force model in turning of LM6/SiCP metal matrix composite. Measurement 47: 452–464